



## Periodic truss structures



Frank W. Zok\*, Ryan M. Lattice, Matthew R. Begley

Materials Department, University of California, Santa Barbara, CA 93106, USA

---

### ARTICLE INFO

**Article history:**

Received 28 August 2015

Received in revised form

15 May 2016

Accepted 5 July 2016

Available online 7 July 2016

---

**Keywords:**

Cellular materials

Structures

---

### ABSTRACT

Despite the recognition of the enormous potential of periodic trusses for use in a broad range of technologies, there are no widely-accepted descriptors of their structure. The terminology has been based loosely either on geometry of polyhedra or of point lattices: neither of which, on its own, has an appropriate structure to fully define periodic trusses. The present article lays out a system for classification of truss structure types. The system employs concepts from crystallography and geometry to describe nodal locations and connectivity of struts. Through a series of illustrative examples of progressively increasing complexity, a rational taxonomy of truss structure is developed. Its conceptual evolution begins with elementary cubic trusses, increasing in complexity with non-cubic and compound trusses as well as supertrusses, and, finally, with complex trusses. The conventions and terminology adopted to define truss structure yield concise yet unambiguous descriptions of structure types and of specific (finite) trusses. The utility of the taxonomy is demonstrated by bringing into alignment a disparate set of ad hoc and incomplete truss designations previously employed in a broad range of science and engineering fields. Additionally, the merits of a particular compound truss (comprising two interpenetrating elementary trusses) is shown to be superior to the octet truss for applications requiring high stiffness and elastic isotropy. By systematically stepping through and analyzing the finite number of structure types identified through the present classification system, optimal structures for prescribed mechanical and functional requirements are expected to be ascertained in an expeditious manner.

© 2016 Elsevier Ltd. All rights reserved.

---

## 1. Introduction

Cellular structures and materials are ubiquitous in biological systems (Wainwright et al., 1982), structural engineering (Evans et al., 2001) and materials science (Gibson and Ashby, 1997). Broadly, they consist of periodic arrays of plate- or strut-like elements. They can be designed to most efficiently exploit the properties of the constituent elements and/or the intervening spaces in achieving functionality, e.g., bearing loads, enabling fluid flow, facilitating heat transfer, altering optical transmission. They are generally superior to structures in which the elements are distributed in a non-periodic manner, e.g. stochastic foams (Evans et al., 2001). In some cases (e.g. photonic materials), periodicity is essential to achieving functionality. For load bearing applications, strut-like elements in particular are preferred: the load for initiating buckling of a slender strut being much higher than that of a comparable plate with the same mass.

Strut-based cellular structures and materials – hereafter collectively referred to as trusses – are under development for

---

\* Corresponding author.

E-mail address: [zok@engineering.ucsb.edu](mailto:zok@engineering.ucsb.edu) (F.W. Zok).

use in an incredibly broad range of technologies, including structural biomedical implants (Murr et al., 2010), aerospace and naval structures (Evans et al., 2001), cushioning and force protection systems (Wadley, 2000), thermal management (Wadley, 2000), actuated structures (Lucato et al., 2004; Hutchinson et al., 2003) and photonic materials (Bückmann et al., 2012; Bauer et al., 2014). Five main classes of fabrication routes have been employed.

- (i) Investment casting has been used to make laboratory-scale Al-alloy truss structures (Deshpande et al., 2001; Chiras et al., 2002; Wallach and Gibson, 2001). Investment casting is generally the most expensive and least amenable to large-scale production relative to other fabrication routes.
- (ii) Fabrication schemes based on conventional machining, bending, assembly and brazing of sheet materials have been devised to make metallic trusses (Wadley, 2000; Rathbun et al., 2004). In one version, diamond-shaped holes are punched or laser-machined into thin steel sheet, leaving an X-pattern of narrow struts. The sheet is then bent along lines of nodes to produce one layer of the targeted truss (Wadley et al., 2003).
- (iii) Metallic trusses can also be made by weaving wires into the desired structure and subsequently brazing the wires together (Wadley, 2000; Kang, 2015). One of the drawbacks is that the weaving operations yield wavy or kinked strut segments between nodes. Moreover, since the nodes are formed by brazing of contacting wires, the integrity of these nodes is likely to be strength-limiting.
- (iv) Additive manufacturing offers the widest range of topology options. Some of the most notable developments in recent years have been in Ti-alloy trusses, produced by selective electron beam melting (EBM) of fine alloy powders, for biomedical implants (Murr et al., 2010, 2011; Cheng et al., 2012; Li et al., 2014). In another arena, direct laser writing by optical lithography has been used to fabricate polymer truss structures with extremely fine-scale (sub-micrometer) features, for potential use in photonic applications (Bückmann et al., 2012; Bauer et al., 2014).
- (v) Self-propagating photocuring (SPPC) of photosensitive polymers has found utility in rapid fabrication of polymer trusses for use in impact mitigation and cushioning systems (Jacobsen et al., 2007a, 2007b, 2008). The main advantage of this process is the short time needed for polymerization (typically less than a minute). One significant limitation is the narrow range of materials that exhibit the requisite physical and chemical properties for SPPC as well as the mechanical properties to produce useful truss structures. It is also restricted to topologies in which all struts intersect one of the external faces. That is, it is inherently a “line-of-sight” curing method.

Despite the broad recognition of the potential of periodic trusses for use in many diverse fields of technology, there are no widely-accepted descriptors of their structure. In the numerous articles on this topic that have appeared in the past two decades, the terminology has been based loosely on descriptions of various polyhedra, but often without explicit connections between truss structure and specific characteristics of the reference polyhedron.

For example, trusses designated as pyramidal are conceptually constructed by placing struts along the four edges of a regular square pyramid at which the triangular faces intersect, but not along the edges of the square base (Evans et al., 2001; Wadley, 2000). Similarly, tetrahedral trusses are formed by placing struts along three non-coplanar edges of a tetrahedron, but not on the other three edges (Wadley, 2000; Rathbun et al., 2004). In other cases, truss structures are constructed by placing struts normal to and at the center of each face of the reference polyhedron (*not* along the edges), e.g. the truncated octahedral truss (Gurtner and Durand, 2014; Weaire, 1996). Elsewhere, truss structures have been described as being “tetrahedral with three-fold symmetry” or “tetrahedral with six-fold symmetry”, without explicit designations of strut locations (Jacobsen et al., 2008).

In some instances, new words have been devised to describe truss structure. The octet truss, for example, derives from a combination of octahedral and tetrahedral. Here struts are placed along all edges of a series of regular octahedra and tetrahedra arranged to fill three-dimensional space (Deshpande et al., 2001). Other truss structures have been described loosely as “fully triangulated”, “bulk cross” (Kang, 2015), “cross I symmetric”, “G6”, “G7”, “dode-thin”, and “hatched” (Murr et al., 2010, 2011; Cheng et al., 2012). These and the preceding designations are re-visited in a later section of this article.

In addition to the vagaries introduced by using polyhedra as the basis of truss designations, the terminology fails to recognize the fundamentally different nature of polyhedra and of trusses. A polyhedron is a three-dimensional solid whose outer boundaries are defined by plane polygons such that the edge of each polygon belongs to one other polygon. A truss, on the other hand, consists of a set of points (or nodal locations) and a set of lines (or struts) joining certain points. Solid geometry alone lacks the structure needed to completely and unambiguously describe truss structure.

Descriptions of trusses have also frequently invoked terms derived from the field of crystallography. Examples include “body centered cubic” and “diamond”. Indeed, the association between nodal positions of trusses and space lattices in crystallography has led to the characterization of trusses as lattice materials, lattice structures or simply lattices. In addition to the unfortunate conflict with the definitions of lattices in the context of crystallography, the terminology (again) fails to recognize the fundamental differences between space lattices and truss structure: A space lattice defines only an array of regularly-spaced points and provides no information about the connectivity of those points (i.e. topology). Therefore, crystallography alone (like solid geometry) lacks the structure needed to describe truss structure.

## 2. Elements of a new language

The principal objective of the article is to present a framework within which trusses can be systematically described and classified. This requires a set of conventions and terminology that, when applied in a consistent manner, yields concise yet unambiguous descriptions of structure types and of specific truss designs. In turn, this goal requires a language of truss structure. As with any language – whether expressed by words in a spoken language or by symbols in mathematics or music – the language of truss structure must have three hierarchical elements: (a) a lexicon of the smallest distinct meaningful elements (or morphemes); (ii) a grammatical system by which the morphemes are combined to form the smallest elements that, in isolation, have practical meaning (*i.e.* words); and (iii) a syntax, or a set of rules by which the ordering of elements is used to convey complex ideas (*i.e.* sentences). The key elements of the proposed language of truss structure are summarized in **Table 1** and detailed in due course. Although seemingly short, the language is capable of describing the many truss structures of current scientific and technological interest.

The language of truss structure is derived from logical descriptors of both the nodal points in space and the connectivity of those points by struts. These descriptors and their organization form the basis for the conventions of the language. The fundamental bases of the proposed conventions and associated terminology are fourfold:

- (i) An elementary cubic truss is constructed by joining nearest-neighbor points of one of the three cubic space lattices with struts.
- (ii) An elementary non-cubic truss is constructed by applying an affine deformation to an elementary cubic truss such that the new nodal locations exhibit symmetry of a different space lattice.
- (iii) A compound truss is constructed by combining two different trusses on a single space lattice, with specified scaling, translational and orientational relationships and that have matching nodes.
- (iv) Complex trusses are constructed by either assigning two or more nodes to each lattice point and then joining nearest-

**Table 1**

The language of truss structure.

<b>Lexicon:</b> Smallest meaningful elements
Operators:      { }: truss designation; ⟨ ⟩: stretch vector; [ ]: translational shift  : separation between trusses; (): rotational transformation;   : nodal location
Variables:      λ: stretch ratio; u, v, w: translations; θ: rotation angle; p, q, r: nodes at lattice point; x, y, z: coordinate axes
Lattices:      SC: simple cubic; BCC: body-centered cubic; FCC: face-centered cubic; SO: simple orthorhombic; BCO: body-centered orthorhombic; ST: simple tetragonal; FCO: face-centered orthorhombic; BCT: body-centered tetragonal; FCT: face-centered tetragonal; R: rhombohedral
<b>Grammar:</b> Elementary trusses formed by combining smallest meaningful elements
Cubic:            { A } where A=SC, BCC or FCC
Non-cubic:        { A }⟨ λ <sub>x</sub> λ <sub>y</sub> λ <sub>z</sub> ⟩ where A=SO, BCO, ST, FCO, BCT or FCT
Arrays:            { nA } <sup>3</sup> , n <sub>x</sub> { n <sub>y</sub> A } <sup>2</sup> , n <sub>x</sub> { n <sub>y</sub> { n <sub>z</sub> A } } where n is number of cells
<b>Syntax:</b> Rules on ordering in defining compound and complex structure types
Compound cubic truss:      { A <sup>(1)</sup> }   { A <sup>(2)</sup> } (without translation/rotation) { A <sup>(1)</sup> }   { A <sup>(2)</sup> } [ u <sup>(2)</sup> v <sup>(2)</sup> w <sup>(2)</sup> ] (θ <sub>x</sub> <sup>(2)</sup> θ <sub>y</sub> <sup>(2)</sup> θ <sub>z</sub> <sup>(2)</sup> ) (with translation/rotation)
Compound cubic supertruss:      { 2A <sup>(1)</sup> }   { A <sup>(2)</sup> }⟨ 2 2 2 ⟩ (without translation/rotation) { 2A <sup>(1)</sup> }   { A <sup>(2)</sup> }⟨ 2 2 2 ⟩ [ u <sup>(2)</sup> v <sup>(2)</sup> w <sup>(2)</sup> ] (θ <sub>x</sub> <sup>(2)</sup> θ <sub>y</sub> <sup>(2)</sup> θ <sub>z</sub> <sup>(2)</sup> ) (with translation/rotation)
Compound non-cubic truss:      { A <sup>(1)</sup> }⟨ λ <sub>x</sub> <sup>(1)</sup> λ <sub>y</sub> <sup>(1)</sup> λ <sub>z</sub> <sup>(1)</sup> ⟩   { A <sup>(2)</sup> }⟨ λ <sub>x</sub> <sup>(2)</sup> λ <sub>y</sub> <sup>(2)</sup> λ <sub>z</sub> <sup>(2)</sup> ⟩ (without translation/rotation) { A <sup>(1)</sup> }⟨ λ <sub>x</sub> <sup>(1)</sup> λ <sub>y</sub> <sup>(1)</sup> λ <sub>z</sub> <sup>(1)</sup> ⟩   { A <sup>(2)</sup> }⟨ λ <sub>x</sub> <sup>(2)</sup> λ <sub>y</sub> <sup>(2)</sup> λ <sub>z</sub> <sup>(2)</sup> ⟩ [ u <sup>(2)</sup> v <sup>(2)</sup> w <sup>(2)</sup> ] (θ <sub>x</sub> <sup>(2)</sup> θ <sub>y</sub> <sup>(2)</sup> θ <sub>z</sub> <sup>(2)</sup> ) (with translation/rotation)
Compound non-cubic supertruss:      { 2A <sup>(1)</sup> }⟨ λ <sub>x</sub> λ <sub>y</sub> λ <sub>z</sub> ⟩   { A <sup>(2)</sup> }⟨ 2λ <sub>x</sub> 2λ <sub>y</sub> 2λ <sub>z</sub> ⟩ (without translation/rotation) { 2A <sup>(1)</sup> }⟨ λ <sub>x</sub> λ <sub>y</sub> λ <sub>z</sub> ⟩   { A <sup>(2)</sup> }⟨ 2λ <sub>x</sub> 2λ <sub>y</sub> 2λ <sub>z</sub> ⟩ [ u <sup>(2)</sup> v <sup>(2)</sup> w <sup>(2)</sup> ] (θ <sub>x</sub> <sup>(2)</sup> θ <sub>y</sub> <sup>(2)</sup> θ <sub>z</sub> <sup>(2)</sup> ) (with translation/rotation)
<i>i</i> translations of same truss type:      { A[ 0 0 0 ][ u <sup>(2)</sup> v <sup>(2)</sup> w <sup>(2)</sup> ]...[ u <sup>(i)</sup> v <sup>(i)</sup> w <sup>(i)</sup> ] }
<i>i</i> nodes at lattice points:      { A[000]   p <sup>(2)</sup> q <sup>(2)</sup> r <sup>(2)</sup> ]...[ p <sup>(i)</sup> q <sup>(i)</sup> r <sup>(i)</sup> ] }

neighbor nodes with struts, or by assembling a number of truss sub-cells to form a super-cell and tiling that super-cell in space.

Hereafter, structure types are denoted by  $\{\dots\}$ , affine (non-distortional) deformations by a stretch vector  $(\lambda_x \lambda_y \lambda_z)$ , translational shifts in origin by  $[u \ v \ w]$ , rotational transformations about the principal axes by  $(\theta_x \theta_y \theta_z)$ , and nodal locations at a lattice point by  $[p \ q \ r]$ . Specific truss configurations further include numerical values  $n$  within  $\{\dots\}$  to indicate the number of unit cells and superscripts  $\beta$  on  $\{\dots\}$  that denote the number of directions in which the truss is tiled in space (1, 2 or 3). Unlike crystallography, where the concepts are predicated on the notion of an infinite array of repeating unit cells, the classification system presented here is not restricted to infinite systems; it naturally allows for the presence of free “boundaries”.

The conventions and terminology are introduced and developed through a series of illustrative examples of progressively increasing complexity; generalizations of the resulting framework and taxonomy are presented afterwards. The hierarchy of the classification system and its conceptual evolution are depicted in Fig. 1. The system begins with elementary cubic trusses (at the center of the figure) and increases in complexity with the introduction of non-cubic and compound trusses and, finally, with complex trusses. The taxonomy is then applied to the descriptions of structure types employed in various science and engineering fields. The merits of one particular compound truss are assessed by comparing the elastic properties of the compound truss with those of the octet truss.

### 3. Development of the language of truss structure

In the present context, trusses are defined as arrays of straight, interconnected struts with periodic character. They can comprise few (large) repeating units, as found in structural engineering, or aggregates of many (small) repeating cells that, collectively, behave essentially as a material. Their structure is defined completely by: (i) the positions of all nodes in space, and (ii) the connectivity of the nodes by struts. Details of node geometry, strut cross-section, strut waviness and other geometric features and defects are not considered.

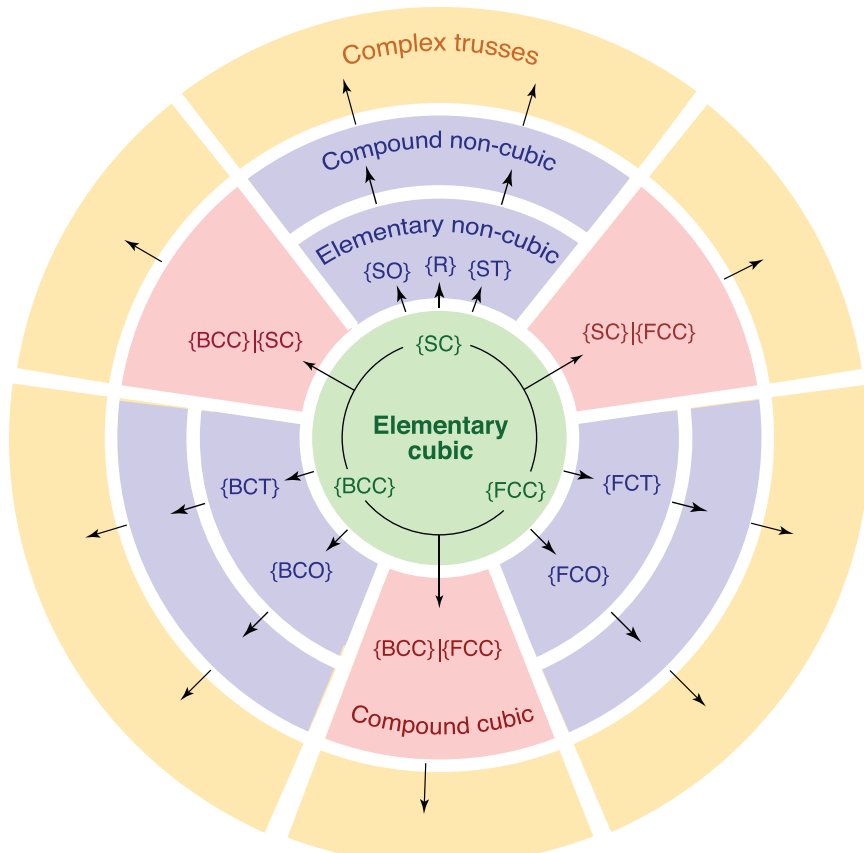


**Fig. 1.** Schematic representation of the structure classification system and its conceptual evolution: from elementary cubic trusses (at the center) to more complex structures with non-cubic symmetries and with multiple constituent trusses in compound systems.

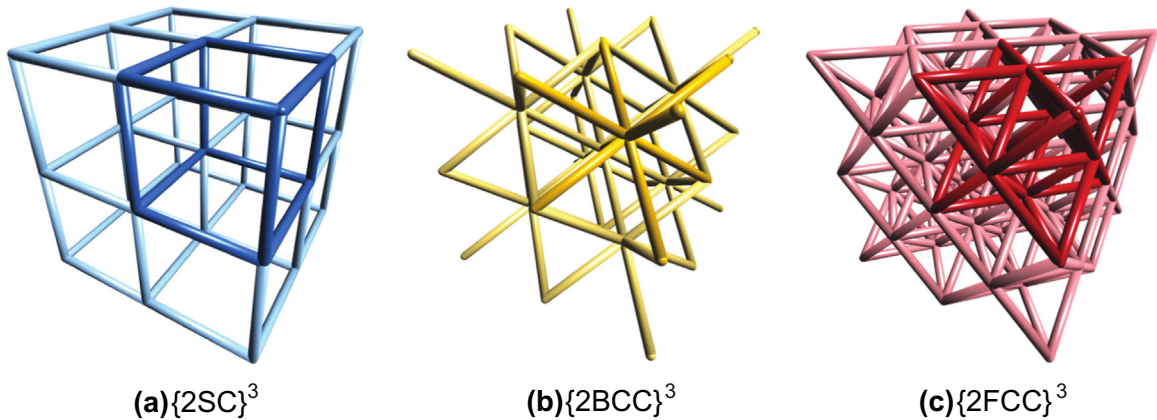


**Fig. 2.** Examples of the three elementary cubic trusses. (Unit cells highlighted by darker colors). (For interpretation of the references to color in this figure legend, the reader is referred to the web version of this article.)

### 3.1. Elementary cubic trusses

By our definition, an elementary cubic truss is constructed by joining pairs of (only) nearest-neighbor points of one of the three cubic space lattices by struts. The complete set of elementary truss types constructed in this manner is illustrated in Fig. 2. The three structure types are denoted simple cubic, {SC}, body-centered cubic, {BCC}, and face-centered cubic, {FCC}. (Here the structure types, indicated by {} brackets, are distinct from those of lattices or crystals.) Any number of unit cells of one truss type, connected at the cell faces, can be tiled to form a truss. The three specific trusses in Fig. 2 consist of  $2 \times 2 \times 2$  arrays of unit cells of {SC}, {BCC} and {FCC} trusses; accordingly, they are denoted  $\{2\text{SC}\}^3$ ,  $\{2\text{BCC}\}^3$  and  $\{2\text{FCC}\}^3$ . Here the superscript (3) on  $\{\dots\}$  indicates the number of directions in which the trusses are tiled in space and the numerical value within the  $\{\dots\}$  brackets indicates the number of unit cells in each direction.

The unit cells can be arranged in other ways, to form rectangular (generally non-cubic) prisms. For example, a  $2 \times 5 \times 5$  array of {SC} cells could be expressed as  $2\{5SC\}$  or, more compactly, as  $2\{5SC\}^2$ , i.e. two layers of a  $5 \times 5$  array of {SC} cells. As another example, a  $2 \times 3 \times 6$  array would be  $2\{3(6SC)\}$ .

In the preceding construction, struts are not placed between non-nearest-neighbor points on the space lattice. Doing so, in some cases, would lead to strut intersections. The problem can be visualized with the {SC} truss; struts added between second nearest-neighbors – along the face diagonals – would intersect at the face centers. Although in principle the problem could be rectified by introducing new lattice points at the intersections, the process would alter the space lattice and unnecessarily complicate the truss description. Moreover, the trusses that would emerge through this procedure would not be unique; they could be constructed by other routes, e.g. via the compound trusses described below.

As with their crystallographic counterparts, each unit cell of an *infinite* array of the three elementary trusses contains a characteristic number,  $j_o$ , of lattice *points*:  $j_o=1$  for {SC},  $j_o=2$  for {BCC} and  $j_o=4$  for {FCC}. By analogy – but now going beyond the realm of crystallography – each unit cell of that infinite array contains a characteristic number,  $b_o$ , of *struts*. For example, in an infinite {SC} truss, there are 12 struts per cell, each shared by four adjoining cells, for a net of  $b_o=3$  struts per cell. Each strut is of length  $\ell = a$  where  $a$  is the edge length of the unit cell (analogous to the lattice parameter in crystallography). In {BCC} trusses there are eight struts per unit cell, each starting at the body center and radiating to one of the eight corners, all wholly contained within that cell; thus  $b_o=8$ . The strut length is  $\ell = \sqrt{3}a/2$ . In an {FCC} cell, there are 12 struts connecting the six face centers, all wholly contained within that cell. There are also four struts joining each face center to the four corners on each of the six cube faces; since each of the latter struts is shared by two adjoining unit cells, collectively they net a total of 12 struts per cell. Combining with the ones joining the face centers yields a total of  $b_o=24$  struts. Each has a length of  $a/\sqrt{2}$ .

Analogous procedures are used to determine the number of struts  $b$  and lattice points  $j$  for systems of finite size. Consider for example multiple unit cells of an elementary truss arranged either as a line of  $n$  cells (joined at their faces), as a square array of  $n \times n$  cells, or as a cubic array of  $n \times n \times n$  cells. The {SC} trusses thus produced are denoted  $\{nSC\}^1$ ,  $\{nSC\}^2$  and  $\{nSC\}^3$ . Analogous terminology would be used to describe {BCC} and {FCC} trusses constructed in this manner. General results for  $b$  and  $j$  of finite trusses are obtained from geometry and are expressed by the simple formulae in Table 2.

A key characteristic of truss topology is the connectivity,  $Z$ , defined as the average number of struts meeting at each node. Since each strut ends at two nodes, the average connectivity is  $Z = 2b/j$ . For infinite trusses,  $Z = Z_0 = 2b_0/j_0$ . The latter takes on values of  $Z_0=6, 8$  and  $12$  for {SC}, {BCC} and {FCC} trusses, respectively. For linear, square and cubic arrays of finite size, the connectivity can be calculated using the expressions for  $b$  and  $j$  in Table 2.

Truss geometry is further characterized by the relative density (or volume fraction)  $\rho$  of strut material within the volume defined by the external boundaries of the truss. When the strut radius  $r$  is small in comparison to the strut length  $\ell$ , the relative density of a unit cell (contained within an infinite truss) is given by  $\rho = \rho_c = \pi b_0(r/a)^2(\ell/a)$ . Expressions for  $\rho$  for

**Table 2**

Geometric characteristics of linear, square and cubic arrays of elementary trusses of finite size.

	{SC}	{BCC}	{FCC}
Linear array of $n$ cells	$b = 8n + 4$ $j = 4n + 4$ $\rho = \pi\left(\frac{r}{a}\right)^2\left(8 + \frac{4}{n}\right)$	$b = 8n$ $j = 5n + 4$ $\rho = 4\sqrt{3}\pi\left(\frac{r}{a}\right)^2$	$b = 32n + 4$ $j = 9n + 5$ $\rho = \frac{\pi}{\sqrt{2}}\left(\frac{r}{a}\right)^2\left(32 + \frac{4}{n}\right)$
Square $n \times n$ array	$b = 5n^2 + 6n + 1$ $j = 2(1+n)^2$ $\rho = \pi\left(\frac{r}{a}\right)^2\left(5 + \frac{6}{n} + \frac{1}{n^2}\right)$	$b = 8n^2$ $j = 3n^2 + 4n + 2$ $\rho = 4\sqrt{3}\pi\left(\frac{r}{a}\right)^2$	$b = 28n^2 + 8n$ $j = 6n^2 + 6n + 2$ $\rho = \frac{\pi}{\sqrt{2}}\left(\frac{r}{a}\right)^2\left(28 + \frac{8}{n}\right)$
Cubic $n \times n \times n$ array	$b = 3n(1+n)^2$ $j = (1+n)^3$ $\rho = \pi\left(\frac{r}{a}\right)^2\left(3 + \frac{6}{n} + \frac{3}{n^2}\right)$	$b = 8n^3$ $j = (1+2n)(1+n+n^2)$ $\rho = 4\sqrt{3}\pi\left(\frac{r}{a}\right)^2$	$b = 12n^2(1+2n)$ $j = (1+n)(1+2n+4n^2)$ $\rho = \frac{\pi}{\sqrt{2}}\left(\frac{r}{a}\right)^2\left(24 + \frac{12}{n}\right)$

systems of finite size have also been derived and are presented in [Table 2](#).

### 3.2. Compound cubic trusses

Deficiencies in connectivity of elementary trusses (discussed below) can be rectified by combining dissimilar elementary trusses to form compound cubic trusses. For example, combining a {2BCC}<sup>3</sup> truss and a {2SC}<sup>3</sup> truss – both residing in the same Cartesian coordinate system with the same origin and the same unit cell edge length – yields the compound truss {2BCC}<sup>3</sup>|{2SC}<sup>3</sup> ([Fig. 3\(a\)](#)). (The vertical line is used to indicate that information on either side pertains to different constituent trusses.) If all strut radii are the same, the relative density of the compound truss is simply the additive sum of the relative densities of the constituent trusses. For example, for an infinite truss of the structure type {BCC}|{SC}, the relative density is  $\rho_o = (4\sqrt{3} + 3)\pi(r/a)^2$ . Similarly, the number of struts is the sum of those in the constituent trusses, i.e.  $b_o = 3 + 8 = 11$ . In contrast, the number of nodes  $j_o$  is not additive. Instead, it is greater of the two values of  $j_o$  of the two trusses, i.e.  $j_o = j_o^{(BCC)} = 2$ . Consequently, the average connectivity is  $Z_o = 2b_o/j_o = 11$ . But the connectivity is not the same at each node:  $Z_o = 8$  for half of the nodes (at the body centers) and  $Z_o = 14$  for the other half (at the body corners).

Recognizing that only half of all lattice points of the {2BCC}<sup>3</sup> truss are used in the construction of the {2SC}<sup>3</sup> truss, a second SC truss with the same edge length could be added. It would differ from the first only in that its origin would reside at the position [1/2 1/2 1/2] (in units of edge length). But, because of the constraints set by the size of the parent truss, only one such unit cell could be added; additional struts emanating from this truss would extend beyond the external boundaries of the parent truss. This particular compound truss is denoted {2BCC}<sup>3</sup>|{2SC}<sup>3</sup>|{SC}|[1/2|21/2] ([Fig. 3\(b\)](#)). The latter part of the designation indicates that the origin of the last in the series of constituent trusses, notably {SC}, is shifted by  $[u v w] = [1/2|21/2]$  with respect to the origin of the parent {BCC} truss. Similarly, large trusses of this type (with  $n > 1$ ) would be denoted {nBCC}<sup>3</sup>|{nSC}<sup>3</sup>|{(n - 1)SC}<sup>3</sup>|[1/2 1/2 1/2]. The structure type is {BCC}|{SC}|{SC}|[1/2 1/2 1/2]. Values of  $Z_o$  for these and other structure types are given in [Table 3](#).

Another example of a compound truss, {2FCC}<sup>3</sup>|{2SC}<sup>3</sup>, is shown in [Fig. 3\(c\)](#). Here, again, the constituent elementary trusses share a common coordinate system and origin. Although the SC truss does not occupy all of the nodes defined by the FCC truss, a third unit cell (e.g., a second SC truss) cannot be introduced into the existing {2FCC}<sup>3</sup>|{2SC}<sup>3</sup> truss without producing strut intersections. For this structure type – {FCC}|{SC} –  $\rho_o$  and  $b_o$  are additive ( $\rho_o = (12\sqrt{2} + 3)\pi(r/a)^2$  and  $b_o = 27$ ),  $j_o = 4$  (that for {FCC}) and the average connectivity is  $Z_o = 13.5$ .

Yet another example of a compound cubic truss, {2FCC}<sup>3</sup>|{2BCC}<sup>3</sup>, is shown in [Fig. 3\(d\)](#). As in the preceding example, no more than one of each of the two truss types can be combined without producing strut intersections. For the {FCC}|{BCC} structure type,  $\rho_o$  and  $b_o$  are (again) additive:  $\rho_o = (12\sqrt{2} + 4\sqrt{3})\pi(r/a)^2$  and  $b_o = 32$ . But, because the {BCC} contributes one additional node at the body center of each cell (not present in the parent {FCC} truss), the number of nodes is  $j_o = 5$  and the connectivity is  $Z_o = 12.8$ .

A variant on the {2FCC}<sup>3</sup>|{2SC}<sup>3</sup> compound truss is shown in [Fig. 4\(a\)](#). It comprises a  $2 \times 2 \times 2$  array of {SC} cells with edge length  $a$  and one {FCC} cell with the same origin but with twice the edge length ( $2a$ ). Conceptually, the {FCC} cell is produced by

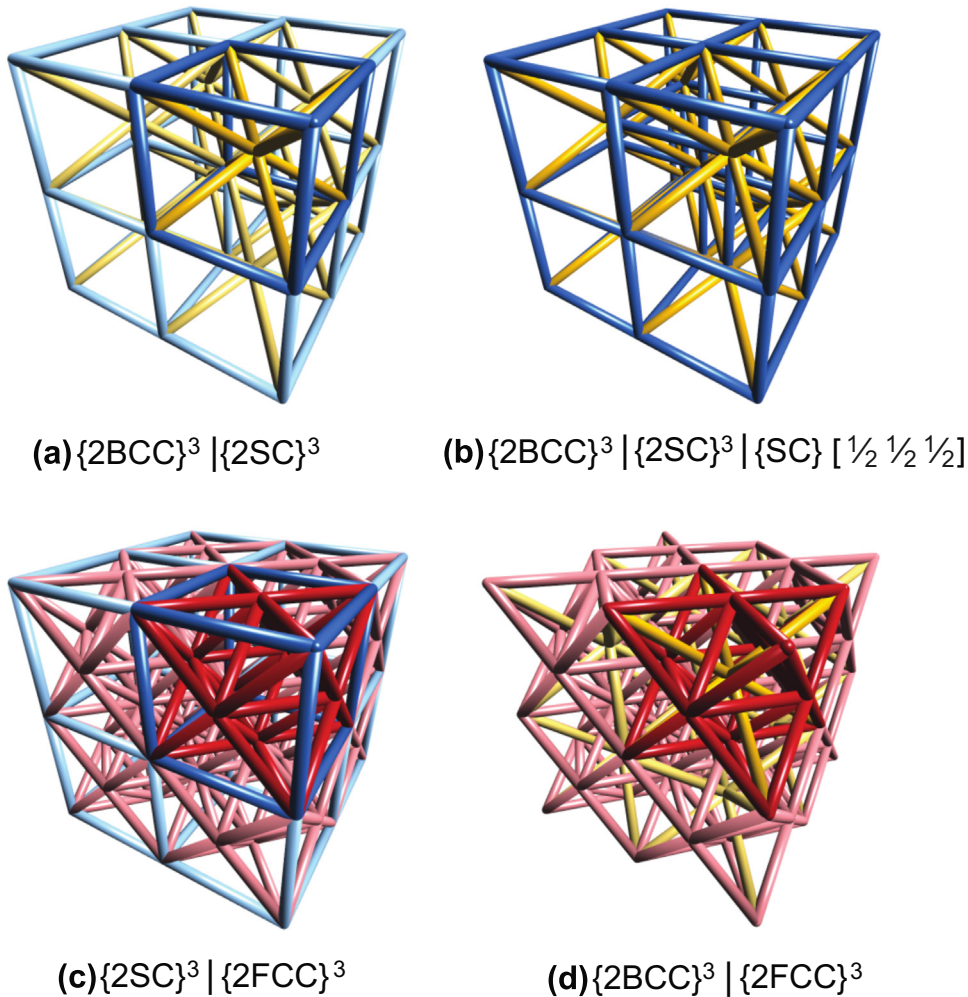


**Fig. 3.** Compound cubic trusses. Unit cells are highlighted by darker colors. (Movies of trusses in (a) and (b) available as Supplementary Material). (For interpretation of the references to color in this figure legend, the reader is referred to the web version of this article.)

scaling the edge lengths of the parent {FCC} truss by a stretch ratio vector  $\langle \lambda_x \lambda_y \lambda_z \rangle = \langle 2 2 2 \rangle$ . The truss is therefore denoted  $\{2SC\}^3 | \{FCC\} \langle 2 2 2 \rangle$ . It represents a cubic supercell that can be duplicated and tiled in space to make larger trusses. Its structure type is  $\{2SC\} | \{FCC\} \langle 2 2 2 \rangle$ . By analogy to superlattices in compound crystals, such collections are called supertrusses. Five other cubic supertrusses are shown in Fig. 4:  $\{2SC\}^3 | \{BCC\} \langle 2 2 2 \rangle$ ,  $\{2SC\}^3 | \{FCC\} \langle 2 2 2 \rangle$ ,  $\{2FCC\}^3 | \{SC\} \langle 2 2 2 \rangle$ ,  $\{2FCC\}^3 | \{BCC\} \langle 2 2 2 \rangle$ ,  $\{2BCC\}^3 | \{FCC\} \langle 2 2 2 \rangle$  and  $\{2BCC\}^3 | \{SC\} \langle 2 2 2 \rangle$  ([Video 1](#), [Video 2](#), [Video 3](#), [Video 4](#), [Video 5](#), [Video 6](#), [Video 7](#), [Video 8](#)).

### 3.3. Non-cubic trusses

An elementary non-cubic truss is constructed by applying an affine deformation to an elementary cubic truss. (This procedure differs from first identifying a non-cubic space lattice and then joining lattice points. In the latter scenario, joining only nearest-neighbor points with struts would generally lead to a non-contiguous truss.) Two examples are shown in Fig. 5. The first is simple orthorhombic {SO}. Here the inter-axis angles are  $90^\circ$  and the edge lengths along the three principal directions differ. It is derived from a {SC} truss through stretching/compressing operations in two of the three principal directions, say  $y$  and  $z$ , e.g.  $\langle \lambda_x \lambda_y \lambda_z \rangle = \langle 1, 1.2, 1.5 \rangle$ . This particular truss is denoted  $\{SO\}^2 \langle 1, 1.2, 1.5 \rangle$  and its structure type is  $\{SO\} \langle \lambda_x \lambda_y \lambda_z \rangle$ .

Because an affine deformation does not alter truss *topology*,  $b_o$ ,  $j_o$  and  $Z_o$  are the same as those of the parent {SC} truss. The relative density, being a characteristic of geometry (not topology), differs. It is readily obtained from geometry.

The second is body-centered orthorhombic {BCO}, constructed by applying two stretching/compressing operations to a {BCC} truss. If the stretch ratio vector is again taken to be  $\langle \lambda_x \lambda_y \lambda_z \rangle = \langle 1, 1.2, 1.5 \rangle$ , the resulting truss would be  $\{BCO\}^2 \langle 1, 1.2, 1.5 \rangle$ . Four other non-cubic structure types with orthogonal axes are possible: face-centered orthorhombic,

**Table 3**  
A summary of structure types.

System	Truss family	Structure type	$Z_o$
Cubic	Elementary <sup>(a)</sup>	{SC} {BCC} {FCC}	6 8 12
	Compound <sup>(a)</sup>	{BCC}   {SC} {BCC}   {SC}   {SC} [½ ½ ½] {FCC}   {BCC} {FCC}   {SC}	11 14 12 ½ 13 ½
	Compound supertruss <sup>(a,b)</sup>	{2SC}   {FCC} <2 2 2> {2SC}   {BCC} <2 2 2> {2FCC}   {SC} <2 2 2> {2FCC}   {BCC} <2 2 2> {2BCC}   {FCC} <2 2 2> {2BCC}   {SC} <2 2 2>	12 8 12 ¾ 12 ½ 14 ¾ 11 ½
Non-cubic	Elementary <sup>(a,c)</sup>	{SO} ⟨λ <sub>x</sub> λ <sub>y</sub> λ <sub>z</sub> ⟩ {BCO} ⟨λ <sub>x</sub> λ <sub>y</sub> λ <sub>z</sub> ⟩ {FCO} ⟨λ <sub>x</sub> λ <sub>y</sub> λ <sub>z</sub> ⟩ {ST} ⟨λ <sub>x</sub> λ <sub>y</sub> λ <sub>z</sub> ⟩ {BCT} ⟨λ <sub>x</sub> λ <sub>y</sub> λ <sub>z</sub> ⟩ {FCT} ⟨λ <sub>x</sub> λ <sub>y</sub> λ <sub>z</sub> ⟩ {R} ⟨λ <sub>111</sub> ⟩	6 8 12 6 8 12 6
	Compound <sup>(d)</sup>	{A <sup>(1)</sup> } ⟨λ <sub>x</sub> λ <sub>y</sub> λ <sub>z</sub> ⟩   {A <sup>(2)</sup> } ⟨λ <sub>x</sub> λ <sub>y</sub> λ <sub>z</sub> ⟩	
	Compound supertruss <sup>(d)</sup>	{2A <sup>(1)</sup> } ⟨λ <sub>x</sub> λ <sub>y</sub> λ <sub>z</sub> ⟩   {A <sup>(2)</sup> } ⟨2λ <sub>x</sub> 2λ <sub>y</sub> 2λ <sub>z</sub> ⟩	
Complex <sup>(e)</sup>	Diamond cubic	{FCC} [0 0 0] [½ ½ ½]	4
	Kagome	{R} [0 0 0] [0 0 ½] [0 ½ 0] [½ 0 0] ⟨λ <sub>111</sub> = √3⟩	6
	Rhombic dodecahedron	{BCC} [0 0 0] [0 1 1] [1 0 1] [1 1 0]	5 ½

<sup>(a)</sup> Structure types within family are comprehensive

<sup>(b)</sup> Only considers truss size ratio of two

<sup>(c)</sup> Neglects trusses with non-orthogonal axes, except for rhombohedral

<sup>(d)</sup> Structure types are generic; A<sup>(i)</sup> are elementary trusses

<sup>(e)</sup> Structure types are illustrative

{FCO}, body-centered tetragonal, {BCT}, simple tetragonal, {ST}, and face-centered tetragonal {FCT}. Here, again,  $b_o$ ,  $j_o$  and  $Z_o$  are the same as those of the parent truss. Excluding trusses with non-orthogonal axes, the preceding list of (six) elementary non-cubic structure types is comprehensive.<sup>1</sup>

Elementary non-cubic trusses can be combined to form compound non-cubic trusses. For example, combining the  $\{2SO\}^2(1, 1.2, 1.5)$  with the  $\{2BCO\}^2(1, 1.2, 1.5)$  yields the truss shown in Fig. 5(c) and denoted  $\{2SO\}^2(1, 1.2, 1.5) | \{2BCO\}^2(1, 1.2, 1.5)$ . Here the coordinate axes and the origins of the two trusses are the same.

Elementary non-cubic trusses can also be combined to form compound non-cubic supertrusses. For example, combining one  $\{2BCO\}^2(1, 1.2, 1.5)$  truss with one  $\{SO\}(2, 2.4, 3)$  truss yields  $\{2BCO\}^2(1, 1.2, 1.5) | \{SO\}(2, 2.4, 1.5)$  (Fig. 5(d)). Here both stretch vectors are referenced to the dimensions of the baseline cubic truss.

Other non-cubic trusses can be formed by applying affine shear deformations to the preceding trusses. One example is the rhombohedral truss, {R}. The rhombohedral truss is of interest for two reasons: (i) it can be readily made by the SPPC process (Jacobsen et al., 2007a, 2007b, 2008) and (ii) it forms the basis for the Kagome truss (described below). Conceptually, it is formed by stretching a {SC} truss along the cube diagonal while maintaining constant strut lengths. In doing so, the inter-axis angles decrease below 90°. An example is shown in Fig. 5(e). The structure type is denoted {R}⟨λ<sub>111</sub>⟩ where ⟨λ<sub>111</sub>⟩ represents the stretch ratio along the body diagonal. When λ<sub>111</sub> = √2, the three inter-axis angles are 60°.

A compound rhombohedral truss can be constructed by combining two identical rhombohedral trusses with one rotated about the body diagonal by π/3. The structure type could be denoted {R}⟨λ<sub>111</sub>⟩ | {R}⟨λ<sub>111</sub>⟩(θ<sub>111</sub> = π/3), where θ<sub>111</sub> is the rotation angle of the second constituent truss, or, more compactly, as {R(θ<sub>111</sub> = 0, π/3)}⟨λ<sub>111</sub>⟩ (Fig. 5(f)). Here the truss type

<sup>1</sup> In comparing the list of elementary trusses that have orthogonal axes to the list of Bravais space lattices that also have orthogonal axes, we find that one of the space lattices – notably, base-centered orthorhombic – does not have a truss counterpart.

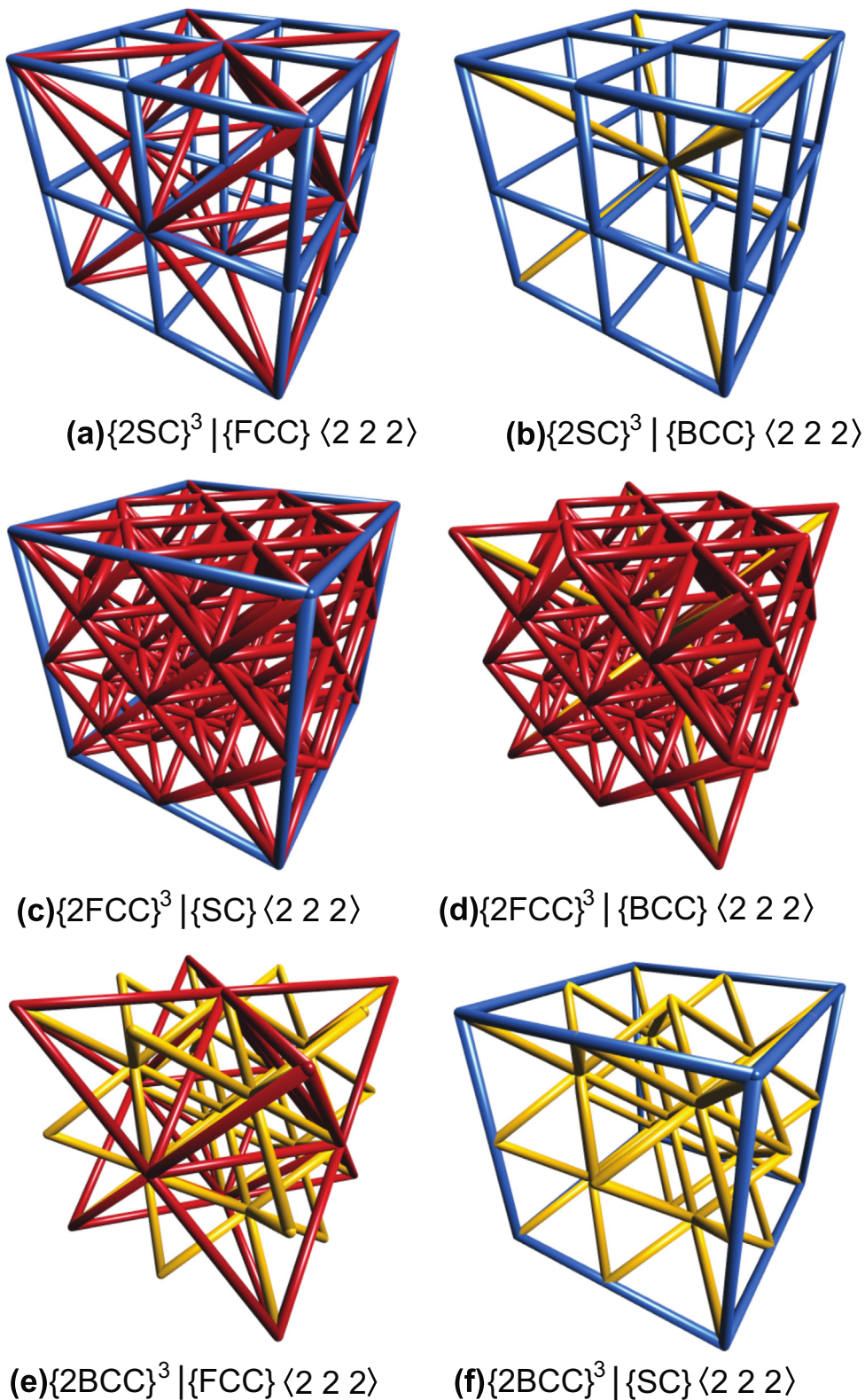
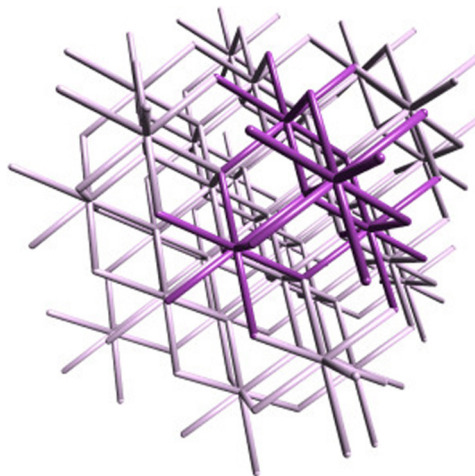
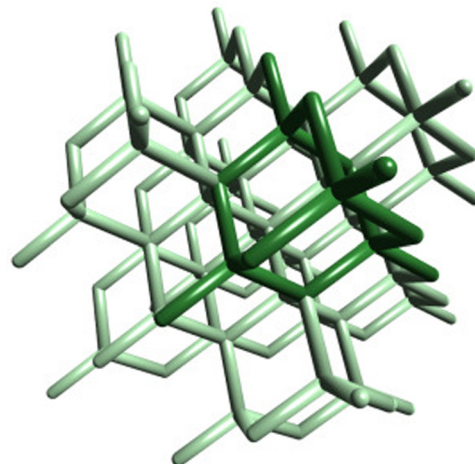


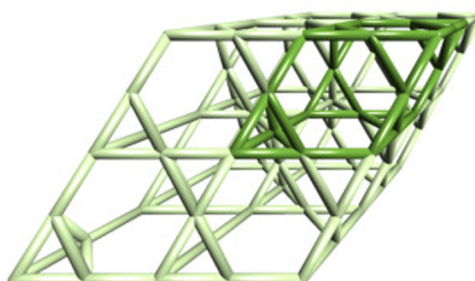
**Fig. 4.** Single unit cells of compound cubic supertrusses. (Movies of trusses in (a), (e) and (f) available as Supplementary material).



**Video 1.** Video of the  $\left\{ 2 \left\{ BCC[0\ 0\ 0][0\ 1\ 1][1\ 0\ 1][1\ 1\ 0] \right\} \right\}^3$  (rhombic dodecahedral) truss. Unit cell is highlighted by darker colors. Supplementary material related to this article can be found online at: <http://dx.doi.org/10.1016/j.jmps.2016.07.007>.

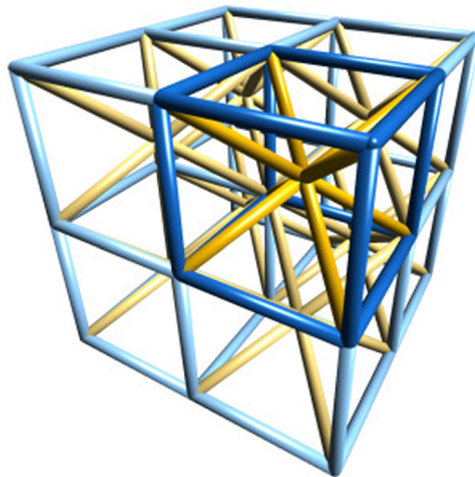


**Video 2.** Video of the  $\left\{ 2 \left\{ FCC[0\ 0\ 0]\left[\frac{1}{4}\frac{1}{4}\frac{1}{4}\right] \right\} \right\}^3$  (diamond cubic) truss. Unit cell is highlighted by darker colors. Supplementary material related to this article can be found online at: <http://dx.doi.org/10.1016/j.jmps.2016.07.007>.

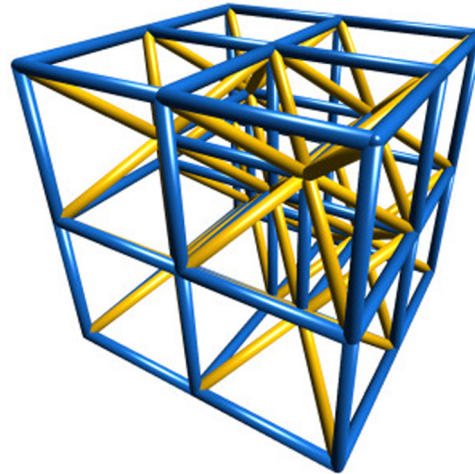


**Video 3.** Video of the  $\left\{ 2 \left\{ R[0\ 0\ 0][0\ 0\ \frac{1}{2}]\left[0\ \frac{1}{2}\ 0\right]\left[\frac{1}{2}\ 0\ 0\right] \right\} \right\}^3$  (Kagome) truss. Unit cell is highlighted by darker colors. Supplementary material related to this article can be found online at: <http://dx.doi.org/10.1016/j.jmps.2016.07.007>.

designation  $R$  is followed by the two rotation angles, all contained within the {} brackets. Compound trusses of this kind have previously been fabricated by SPPC ([Jacobsen et al., 2008](#)).



**Video 4.** Video of the  $\{2BCC\}^3|\{2SC\}^3$  truss. Unit cell is highlighted by darker colors. Supplementary material related to this article can be found online at: <http://dx.doi.org/10.1016/j.jmps.2016.07.007>.



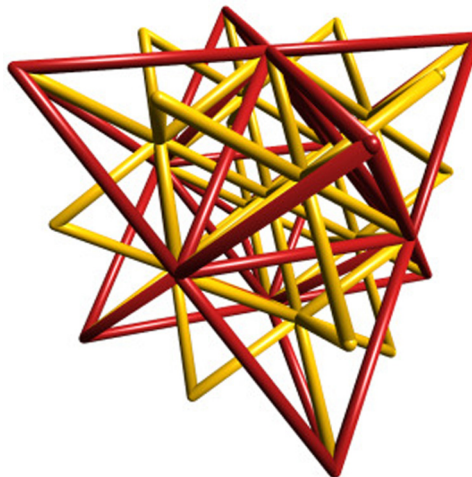
**Video 5.** Video of the  $\{2BCC\}^3|\{2SC\}^3|\{SC\}\left[\frac{1}{2} \frac{1}{2} \frac{1}{2}\right]$  truss. Supplementary material related to this article can be found online at: <http://dx.doi.org/10.1016/j.jmps.2016.07.007>.

Although many other non-cubic trusses could be constructed by applying shear deformations to simpler trusses, the merits of doing so are presently unclear. In most cases the resulting trusses would exhibit low degrees of symmetry and complex shear/normal coupling of stresses and strains. Whether these can be exploited in a useful way in load-bearing systems remains to be established.

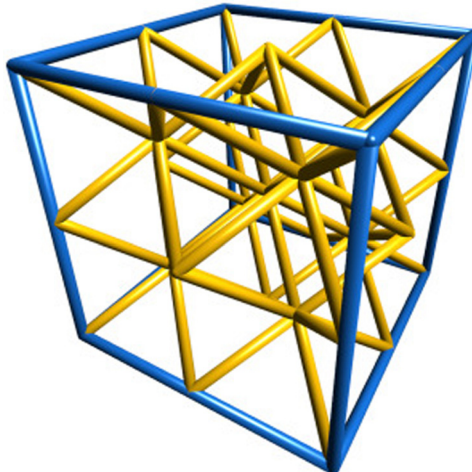
Yet other types of compound non-cubic trusses can be constructed by combining 2D planar trusses with 3D trusses. Conceptually, 2D trusses are constructed by joining nearest neighbor points on a planar (rather than space) lattice with struts. For example, the 2D analogs to {SC} and {ST} (3D) trusses are square {Sq} and rectangular {Re}, respectively. Two examples of compound 2D/3D trusses are shown in Fig. 6. In the first, a  $\{2BCC\}^3$  truss (from Fig. 2(b)) is combined with two square trusses, one on each of two opposing faces. The compound layered truss is denoted  $\{2Sq\}^2|\{2BCC\}^3|\{2Sq\}^2$  and its structure type is  $\{Sq\}|\{BCC\}|\{Sq\}$ . Although in this case the two trusses share common edge lengths and coordinate systems, various scalings, translations and rotations can also be employed. Trusses of this type, with planar trusses on the two external faces of a 3D truss, have been considered for use as stiff, lightweight “sandwich” panels: the 2D trusses serving as the panel faces and the 3D truss as the core. [Wicks and Hutchinson \(2001\)](#): a variant is produced by inserting a third square truss along the mid-plane. This yields a  $\{2Sq\}^2|\{2BCC\}^2|\{2Sq\}^2|\{2BCC\}^2|\{2Sq\}^2$  truss.

### 3.4. Complex trusses

More complex trusses can be constructed following one of two approaches. In the first, two or more nodes are assigned to each point of a space lattice and struts are then placed between nearest-neighbor nodal locations. (The analogy in



**Video 6.** Video of a single unit cell of the  $\{2BCC\}^3 \{ FCC \} \langle 2\ 2\ 2 \rangle$  compound cubic supertruss. Supplementary material related to this article can be found online at: <http://dx.doi.org/10.1016/j.jmps.2016.07.007>.



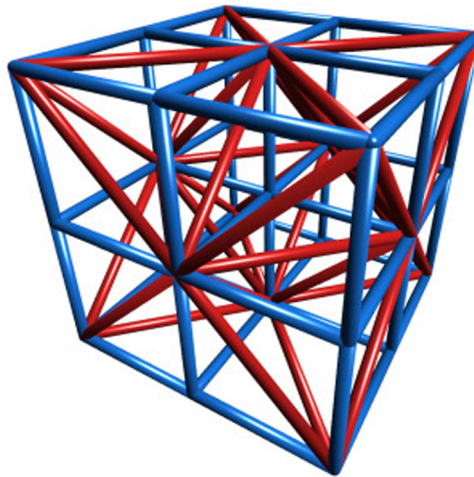
**Video 7.** Video of a single unit cell of the  $\{2BCC\}^3 \{ SC \} \langle 2\ 2\ 2 \rangle$  compound cubic supertruss. Supplementary material related to this article can be found online at: <http://dx.doi.org/10.1016/j.jmps.2016.07.007>.

crystallography is the construction of a crystal structure by placing atom motifs at each point of a space lattice.) Two particular structures of this type have received attention over the years: the diamond cubic truss (Kraft, 1961; Gilman, 1984) and the Kagome truss (Deshpande et al., 2001).

The diamond cubic crystal structure is based upon an *FCC* space lattice with two atoms at each lattice point: at  $[0\ 0\ 0]$  and  $[1/4\ 1/4\ 1/4]$  with respect to the origin of the lattice and at corresponding points following face-centering translations. (Note the use of  $\lfloor \rfloor$  brackets to denote atomic positions at a lattice point) Nodal locations of a diamond cubic truss are defined in the same way. That is, two nodes are assigned to each point of an *FCC* lattice, at  $[0\ 0\ 0]$  and  $[1/4\ 1/4\ 1/4]$ . The truss is formed by joining the nearest-neighbor nodes with struts. The resulting truss comprises tetrahedral-like sub-units<sup>2</sup> with four struts meeting at each node and each strut making an angle of  $109.5^\circ$  to each of the other struts (Fig. 7(a)). The structure type is denoted  $\{FCC[0\ 0\ 0][1/4\ 1/4\ 1/4]\}$ . Here the space lattice designation, *FCC*, is followed by the two nodal locations associated with each lattice point, all contained within the  $\{ \}$  brackets. Its connectivity is  $Z_0 = 4$  at all nodes: the minimum possible value for a three-dimensional truss.

3D Kagome trusses are constructed in a similar way. This truss (Fig. 7(b)) is based upon a rhombohedral space lattice in which the three inter-axis angles are  $60^\circ$ ; the stretch ratio along the body diagonal needed to achieve this angle is  $\lambda_{111} = \sqrt{2}$ . Four nodes are assigned to each lattice point, at  $[0\ 0\ 0]$ ,  $[1/2\ 0\ 0]$ ,  $[0\ 1/2\ 0]$  and  $[0\ 0\ 1/2]$ . Once again, the truss is

<sup>2</sup> The tetrahedral designation comes from the fact that the four struts in each sub-unit are normal to the faces of a regular tetrahedron centered on the nodal point. In other contexts (Wadley, 2000), the tetrahedral designation has been used to describe trusses in which the struts are coincident with the edges of a regular tetrahedron. The two resulting structures are vastly different from one another.



**Video 8.** Video of a single unit cell of the  $\{2SC\}^3|\{FCC\}\langle 2\ 2\ 2\rangle$  compound cubic supertruss. Supplementary material related to this article can be found online at: <http://dx.doi.org/10.1016/j.jmps.2016.07.007>.

constructed by joining the nearest-neighbor nodes with struts. The resulting structure type is  $\{R [0\ 0\ 0]\ [1/2\ 0\ 0]\ [0\ 1/2\ 0]\ [0\ 0\ 1/2]\}\langle\lambda_{111} = \sqrt{2}\rangle$ . As with the preceding designation of the diamond cubic truss, the nodal locations associated with each lattice point are contained within the {} brackets.

In the second approach to constructing complex trusses, a super-cell is first constructed from an assemblage of two or more elementary sub-cells and the super-cell is then duplicated and tiled in three dimensions. (In this context, assemblage refers to a collection of sub-cells that are joined on their faces; it differs from a compound truss, wherein two or more constituent trusses are built on the same space lattice) An illustrative example is a truss based on the rhombic dodecahedron.

The rhombic dodecahedron consists of 12 congruent faces, each in the shape of a rhombus in which the ratio of the long diagonal length to short diagonal length is  $\sqrt{2}$ . It is of interest because it is one of the few polyhedra with congruent faces that can be tiled to fill three-dimensional space. The truss is created by placing struts along each of the edges of the reference polyhedron (Fig. 7(c)). The resulting structure is equivalent to one-half of a {BCC} truss. Conceptually, it can be constructed by alternating one {BCC} cell with one vacant cubic cell in each of the three directions, in a 3D checkerboard pattern. The full unit cell comprises a  $2 \times 2 \times 2$  array of sub-cells: four {BCC} cells and four vacant cubes. The structure type is denoted  $\{BCC [000]\ [011]\ [101]\ [110]\}$ . The four translation vectors within the {} brackets imply four families of {BCC} trusses. Its packing density is  $\rho_0 = (3\sqrt{3}\pi/2)(r/\ell)^2$ . Half of the nodes have connectivity  $Z_0 = 4$  and the other half have  $Z_0 = 8$ ; thus the average value is  $\bar{Z}_0 = 6$ .

#### 4. Generalizations of designations of trusses and structure types

Building upon the pattern established in the preceding examples, a generic terminology is readily developed. As demonstrated in a subsequent section, the terminology can be applied unambiguously to descriptions and classifications of periodic trusses. A summary of the taxonomy is presented in Table 3.

An elementary truss consisting of a linear, square or cubic array of cells is expressed generically as  $\{nA\}^\beta$  where  $A$  is the truss type (*SC*, *BCC* or *FCC*),  $n$  is the number of unit cells in each row and  $\beta$  is the number of directions in which the truss is tiled (1, 2 or 3). The structure type is simply  $\{A\}$ . When combined with the normalized strut radius  $r/a$ , the truss designation completely defines the structure and the geometry of an elementary truss. With these, all other important characteristics ( $b$ ,  $j$ ,  $Z$ ,  $\rho$ ) are known.

When the unit cells are arranged to form other types of rectangular (non-cubic) prisms, the trusses are expressed as  $n_x\{n_y\{n_zA\}\}$  where  $n_x$ ,  $n_y$  and  $n_z$  are the numbers of cells in the  $x$ ,  $y$  and  $z$  directions, respectively. In cases where two of these quantities are equal, say  $n_y=n_z$ , the notation can be contracted to  $n_x\{n_yA\}^2$ .

An elementary non-cubic truss is expressed as  $\{nA\}^\beta\langle\lambda_x\ \lambda_y\ \lambda_z\rangle$  where  $\langle\lambda_x\ \lambda_y\ \lambda_z\rangle$  is the stretch vector required to transform the starting elementary cubic truss to the non-cubic truss  $\{A\}$ . The structure type is  $\{A\}\langle\lambda_x\ \lambda_y\ \lambda_z\rangle$ . Here, again, the truss designation along with  $r/a$  fully define truss structure and geometry. Shearing operations can also be applied; the pertinent strains would then be added to (or replace) the stretch vector.

A compound truss is described by a list of constituent trusses and their relationships with one another. The first truss in the list is the parent; it defines the size, shape and orientation of the system. The spatial extent of the trusses that follow in

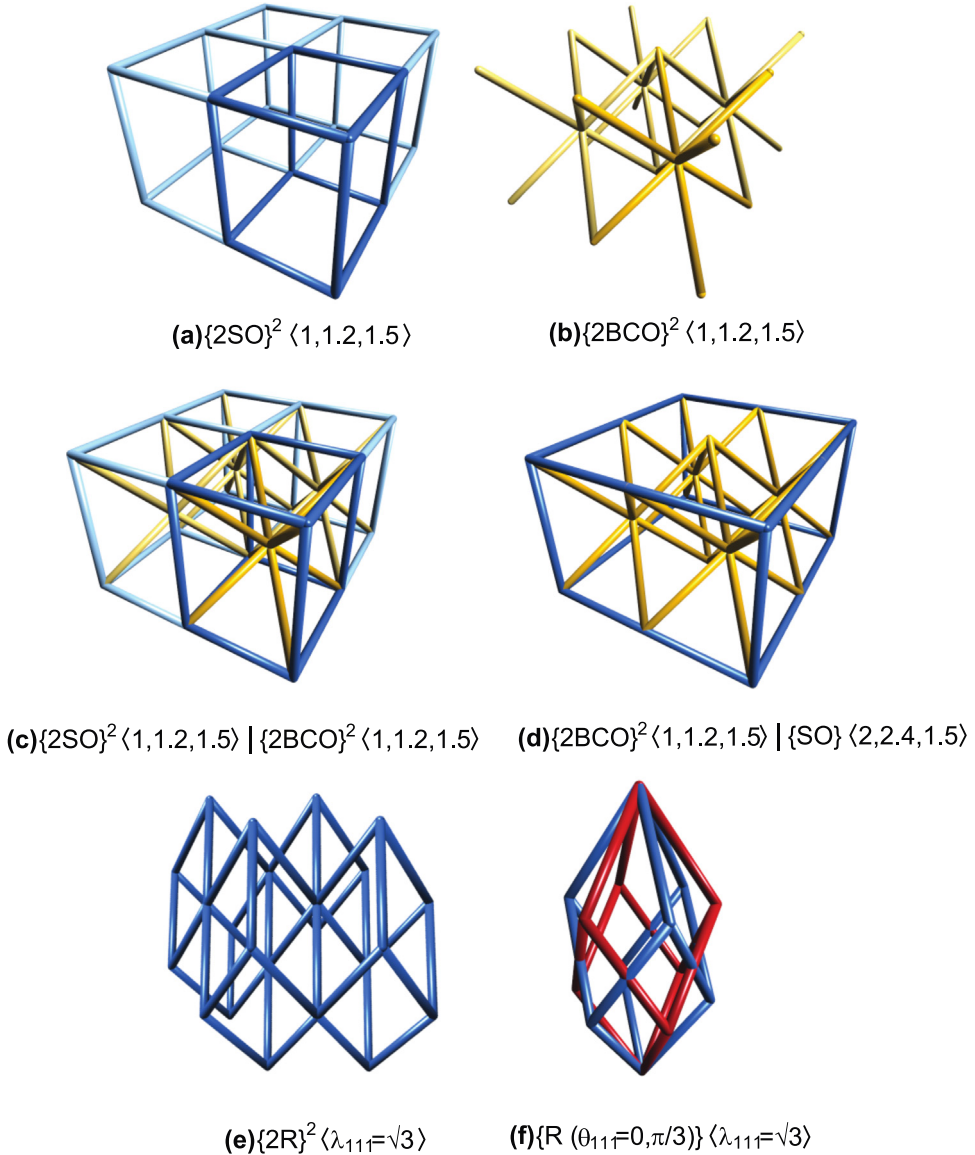


**Fig. 5.** Examples of elementary and compound non-cubic trusses. (A movie of the truss in (e) available as Supplementary material).

the list is restricted to that of the first. Each truss designation is followed, in order, by the stretch vector  $\langle \lambda_x \lambda_y \lambda_z \rangle$ , the translation vector  $[u v w]$ , and the rotations  $(\theta_x \theta_y \theta_z)$  about the coordinate axes, all with respect to the cubic parent. Since the parent truss defines orientation and position, both  $[u v w]$  and  $(\theta_x \theta_y \theta_z)$  for the parent are (usually) identically zero; the stretch vector  $\langle \lambda_x \lambda_y \lambda_z \rangle$  is present only if the parent is non-cubic. When terms are absent, their values are implied to have no effect, e.g., stretch values of unity or rotations of zero. This allows for short designations for simple trusses; additional details are provided only when necessary. In general, a compound truss designation would read as  $\{n^{(1)}A^{(1)}\}^\beta \langle \lambda_x^{(1)} \lambda_y^{(1)} \lambda_z^{(1)} \rangle \left| \{n^{(2)}A^{(2)}\}^\beta \langle \lambda_x^{(2)} \lambda_y^{(2)} \lambda_z^{(2)} \rangle [u^{(2)} v^{(2)} w^{(2)}] (\theta_x^{(2)} \theta_y^{(2)} \theta_z^{(2)}) \right| \dots$  where the superscripts (1), (2),... denote truss family types. If both trusses are cubic, the structure type is  $\{A^{(1)}\} \left| \{A^{(2)}\}\right.$

Compound cubic supertrusses are expressed as  $\{2nA^{(1)}\}^\beta \left| \{nA^{(2)}\}^\beta \langle 2 2 2 \rangle \right.$ . The factor of 2 on the first truss indicates that the ratio of numbers of the two truss types must be  $2^\beta$ ; the stretch ratio  $\langle 2 2 2 \rangle$  on the second truss indicates that the size ratio of the two unit cells is two. The structure type is  $\{2A^{(1)}\} \left| \{A^{(2)}\} \langle 2 2 2 \rangle \right.$ . If deemed to be important, other size and number ratios as well as translations and rotations could be introduced.

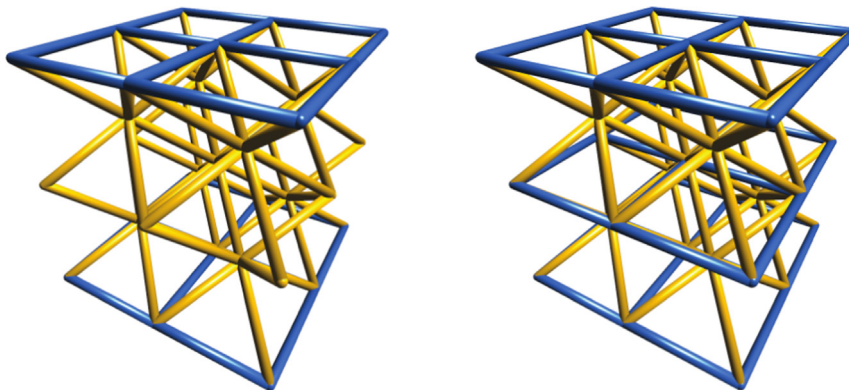


**Fig. 6.** Examples of 2D/3D compound trusses.

More-complex trusses can be constructed by assigning multiple nodes to each lattice point and joining the nearest-neighbor nodes by struts. The structure type is  $\{A|0\ 0\ 0\} [p^{(2)}\ q^{(2)}\ r^{(2)}] \dots [p^{(i)}\ q^{(i)}\ r^{(i)}]$  where  $[p^{(i)}\ q^{(i)}\ r^{(i)}]$  represents the location of the  $i$ th node at each lattice point. Alternatively, a super-cell can be made from an assemblage of elementary sub-cells and the super-cell duplicated and tiled in space. If all of the sub-cells are the same (apart from vacant cells), the structure type would be  $\{A|0\ 0\ 0\} [u^{(2)}\ v^{(2)}\ w^{(3)}] \dots [u^{(i)}\ v^{(i)}\ w^{(i)}]$ .

## 5. Applications

The many disparate truss designations introduced in prior literature can be concisely and unambiguously described using the present system of classification and taxonomy. For example, a pyramidal truss, which contains struts aligned along the four edges at which the triangular faces of a regular square pyramid intersect, is, in general, of the structure type  $\{BCT\}(1\ 1\ \lambda_z)$ , where the base of the  $\{BCT\}$  unit cell coincides with the pyramid base. From geometry, the stretch ratio (measured perpendicular to the pyramid base, or  $z$ -plane) is  $\lambda_z = \sqrt{2} \tan \theta$  where  $\theta$  is the angle between the triangle edges and the square base. (This structure type reduces to a  $\{BCC\}$  for the special case in which  $\lambda_z = 1$  and hence  $\theta = \tan^{-1}(1/\sqrt{2}) \approx 35.26^\circ$ ). Two specific versions of these trusses have been described as “two-layer pyramidal” and “one-layer pyramidal” (Hammetter et al., 2012; Bernal-Ostos et al., 2012); they are, respectively,  $\{nBCT\}^2(1\ 1\ \lambda_z)$  and  $1/2\{nBCT\}^2(1\ 1\ \lambda_z)$ . This structure has also been described as “octahedral-type” (Jacobsen et al., 2008). These and other structure types are summarized in Table 4.

Hierarchical truss designs based on the preceding structure have been synthesized (Doty et al., 2012). They comprise a single-layer pyramidal truss and a fine scale “octahedral-type” truss. Despite the differing descriptions, both trusses are of the type  $\{BCT\}(1, 1, \lambda_z)$ . When combined, the two trusses form a supertruss of the type  $\{BCT\}(1\ 1\ \lambda_z) + \{1/\alpha BCT\}(\alpha\ \alpha\ \alpha\lambda_z)$  where  $\alpha$  is the size ratio of the constituent trusses (large/small). The specific one reported in (Doty et al., 2012) is  $5\{10nBCT\}^2(1\ 1\ \lambda_z) + 1/2\{nBCT\}^2(10\ 10\ 10\lambda_z)$  with  $\lambda_z \approx 3.7$ . That is, it consists of 5 layers of a  $10n \times 10n$  array of  $\{BCT\}(1\ 1\ \lambda_z)$  cells and one half of the full thickness of an  $n \times n$  array of  $\{BCT\}(10\ 10\ 10\lambda_z)$  cells.

A tetrahedral truss, which has struts aligned along three non-coplanar edges of a regular tetrahedron, is of the type  $\{R\}\langle\lambda_{111}\rangle$ . When in the form of a single tetrahedral layer (typically used as cores within sandwich panels), the specific structure is  $1/3\{nR\}^2\langle\lambda_{111}\rangle$ , i.e. one third of the full thickness of an  $n \times n$  array of  $\{R\}\langle\lambda_{111}\rangle$  cells.

The octet truss, comprising struts along the edges of regular octahedra and tetrahedral (Deshpande et al., 2001), is simply  $\{FCC\}$ .

One class of trusses made by SPPC has been described as “tetrahedral with three-fold symmetry” (Jacobsen et al., 2008). This is also of the type  $\{R\}\langle\lambda_{111}\rangle$ . The specific designation depends on the pattern of apertures used for guiding the UV light into the monomer bath and the axes of the three light beams. In the cases described by Jacobsen et al. (2007b), the apertures are in a hexagonal pattern, the projections of the light beams on the mask are at  $120^\circ$  to one another, and each projection is aligned with one of the close-packed directions of the aperture array. As noted earlier, the resulting structure comprises three interlaced but not interconnected  $\{R\}$  trusses. Taking the long axis of the rhombohedra to be aligned with the  $c$ -axis in a hexagonal coordinate system and using the three-index Miller notation, the structure type would be described as  $\{R\}[0\ 0\ 0][0\ 1\ 0][1\ 0\ 0]\langle\lambda_{111}\rangle$ .

A related class of trusses previously described as “tetrahedral with six-fold symmetry” are made in a similar manner but now with six (rather than three) light beams, each with its projection on the mask aligned with one of the six close-packed

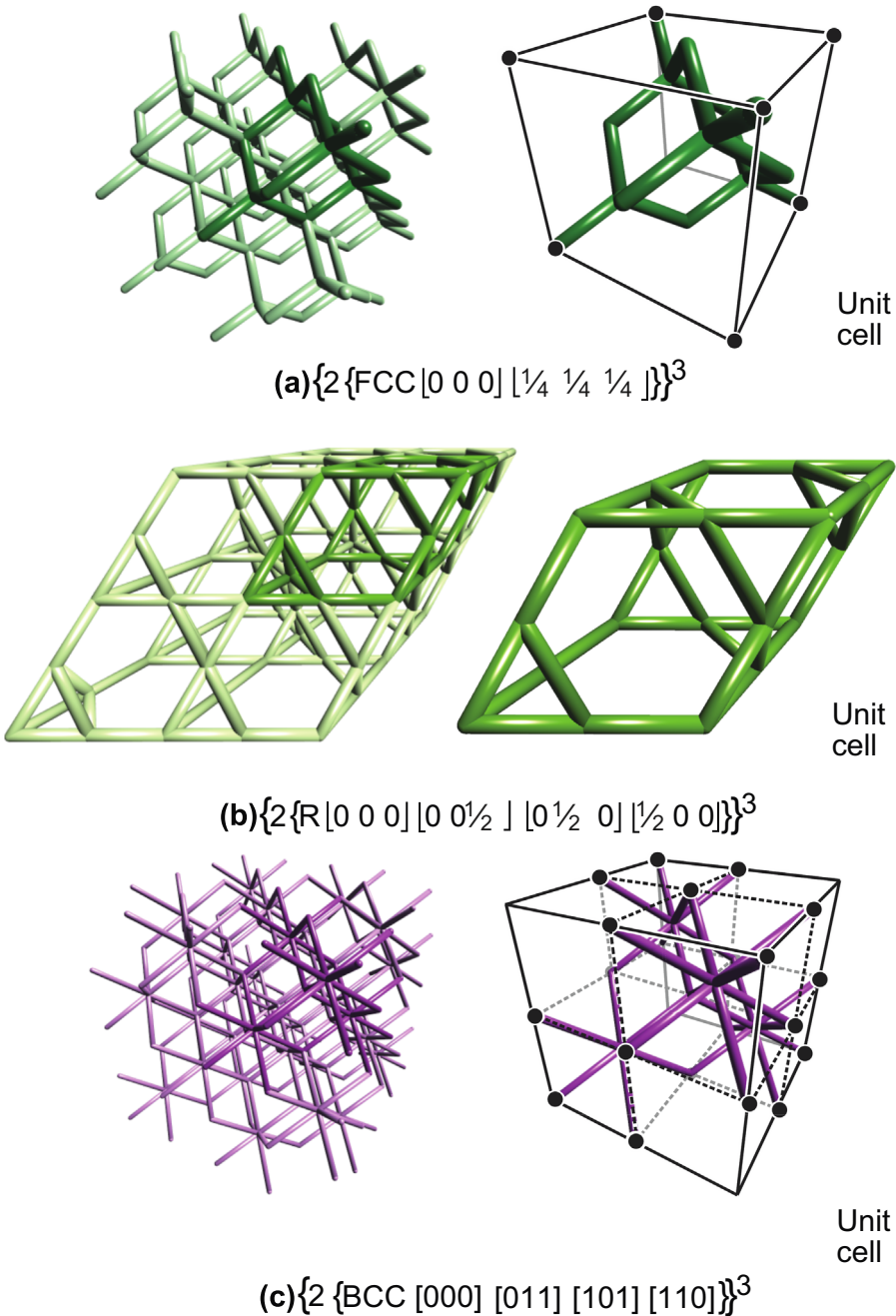


**Fig. 7.** Examples of complex trusses: (a) diamond cubic, (b) Kagome and (c) rhombic dodecahedral. Unit cells are highlighted by darker colors. (Movies of all trusses available as Supplementary material). (For interpretation of the references to color in this figure legend, the reader is referred to the web version of this article.)

directions of the aperture array (Jacobsen et al., 2008). It would be denoted  $\{R [0\ 0\ 0]\ [0\ 1\ 0]\ [1\ 0\ 0]\}(\theta_{111} = 0,\ \pi/3)\langle\lambda_{111}\rangle$  where  $\theta_{111}$  is the rotation about the body diagonal. The two rotations,  $\theta_{111} = 0$  and  $\pi/3$ , imply two families of trusses, each described in full by the contents in the preceding {} brackets and each subjected to a stretch ratio  $\lambda_{111}$  along the body diagonal.

The structures being explored in the medical implant community are based on variants of {SC} (e.g., “cross I symmetric”, “G6”), {BCC}||{Sq} compound trusses (“G7”), or {BCC[000] [011] [101] [110]} (“dode thin” or “rhombic dodecahedral”).

Sandwich panels with planar trusses as “face sheets” and 3D trusses as cores are also conveniently described as compound trusses. One example, previously described as “single layer pyramidal” (Kang, 2015) consists of a pyramidal core,

**Table 4**

Designations of previously-studied trusses.

Reported description	Structure type (according to present taxonomy)	Comments
“G6” (Murr et al., 2010, 2011; Cheng et al., 2012; Li et al., 2014) “Orthotropic with cubic cells” (design C) (Bauer et al., 2014)	{SC}	
“Octahedral-type” (Jacobsen et al., 2007a, 2007b, 2008), “Pyramidal” (Hammetter et al., 2012; Bernal-Ostos et al., 2012)	{BCC} or {BCT}{1 1 λ <sub>z</sub> }	Truss type dictated by strut angle Two-layered: {BCT}{1 1 λ <sub>z</sub> } One-layered: 1/2{BCT}{1 1 λ <sub>z</sub> }
“Octet truss” (Deshpande et al., 2001)	{FCC}	
“Cross I symmetric” (Murr et al., 2010, 2011; Cheng et al., 2012; Li et al., 2014)	{SC}[1/21/21/2]	Same as G6, except for origin translation
“Hatched” (Murr et al., 2010, 2011; Li et al., 2014)	{ST}{1 1 λ <sub>z</sub> }	λ <sub>z</sub> ≈ 1.5
“Tetrahedral” (Wadley, 2000; Rathbun et al., 2004)	1/3{R}{λ <sub>111</sub> }	
“G7” (Murr et al., 2010, 2011; Cheng et al., 2012; Li et al., 2014)	{BCC} {Sq}	
“Body centered cubic” (Pettermann and Husing, 2012)	{BCC} {SC}	
“Orthotropic with cubic cells and global diagonal bracing” (design A) (Bauer et al., 2014)	{2SC} {FCC}{222}	Specific truss tested: {4SC} <sup>3</sup>  {2FCC} <sup>3</sup> {222}
“Dode thin” (Murr et al., 2010, 2011; Cheng et al., 2012; Li et al., 2014)	{BCC}[000][011][101][110]	Also called rhombic dodecahedral
“Tetrahedral with three-fold symmetry” (Jacobsen et al., 2007a, 2007b, 2008)	{R}[0 0 0][0 1 0][1 0 0]{λ <sub>111</sub> }	Based on reported angles λ <sub>111</sub> ≈ √2. Translations [100] and [010] are in the hexagonal coordinate system using three-index Miller notation.
“Tetrahedral with six-fold symmetry” (Jacobsen et al., 2007a, 2007b, 2008)	{R}[0 0 0][0 1 0][1 0 0]{(θ <sub>111</sub> = 0, π/3)}{λ <sub>111</sub> }	Based on reported angles, λ <sub>111</sub> ≈ √2. Superposition of the two {R} trusses lead to strut intersections.
“Regular truncated octahedron” (Gurtner and Durand, 2014), “Reinforced body centered cubic” (Pettermann and Husing, 2012)	{BCC} {SC} {SC}[1/21/21/2]	
Hierarchical “single-layer pyramidal truss and octahedral-type truss” (Doty et al., 2012)	{BCT}{1 1 λ <sub>z</sub> }   {1/aBCT}{α α aλ <sub>z</sub> } where α is the size ratio	
“Single-layer pyramidal” (Kang, 2015)	{Sq} 1/2{BCT}{1 1 λ <sub>z</sub> }   {Sq}	Sandwich panel
“Octet panel” (Wicks and Hutchinson, 2001)	{Tr}   1/3{R}{λ <sub>111</sub> = √3}   {Tr}	Sandwich panel

specifically  $1/2\{BCT\}^2\langle 1 1 \lambda_z \rangle$ , and square 2D trusses on each of the two faces. The structure type is  $\{Sq\} | 1/2\{BCT\}\langle 1 1 \lambda_z \rangle | \{Sq\}$ . The form of this designation, with planar trusses “book-ending” a 3D truss, indicates the plate-like character of the structure.

Another sandwich panel was previously described as being an octet truss plate (Wicks and Hutchinson, 2001). It is, loosely, of the structure type {FCC}. But this designation alone is incomplete; it lacks information about the orientation of the truss with respect to the plane of the panel and does not explicitly acknowledge its plate-like character. The structure is best described in terms of its constituent elements: (i) the two faces, each comprising an equilateral triangular arrangement of struts, denoted {Tr}; and (ii) the central core, which is a tetrahedral truss and is denoted here as  $1/3\{R\}\langle\lambda_{111} = \sqrt{3}\rangle$ . Combining, the structure type of the sandwich panel becomes  $\{Tr\} | 1/3\{R\}\langle\lambda_{111} = \sqrt{3}\rangle | \{Tr\}$ . Here, as in the preceding example, the form of the designation immediately marks the structure as being plate-like.

The final example comes from a recent theoretical study of the truss structure that yields the maximum stiffness while retaining isotropic elastic properties. The truss is based on the regular truncated octahedron (also known as the Kelvin cell) (Gurtner and Durand, 2014). This polyhedron has six square faces and eight regular hexagonal faces. The corresponding truss comprises 14 struts emanating from the center, each normal to one of the 14 faces. The structure can be broken down into two interlaced {SC} trusses and one {BCC} truss (Fig. 3(b)). It is equivalent to the compound truss  $\{nBCC\}^3|\{nSC\}^3|(\{n - 1\}SC)^3[1/21/21/2]$ , introduced in Section 3.2. This structure type,  $\{BCC\}|{SC}|{SC}[1/21/21/2]$ , has also been referred to as “reinforced body-centered cubic” (Pettermann and Husing, 2012).

**Table 5**  
Elastic properties.

	$E_l/\rho E_0$	$\nu_{12}$	$G_{12}/\rho E_0$	$\omega \equiv 2G_{12}(1 + \nu_{12})/E_l$
$\{nBCC\}^3   \{nSC\}^3$	0.162	0.257	0.069	1.05
$\{nFCC\}^3$	0.111	0.333	0.083	2.00

## 6. Merits of compound trusses

To illustrate the merits of compound trusses, we compare the elastic properties of two truss types:  $\{nFCC\}^3$  and  $\{nBCC\}^3 | \{nSC\}^3$ . The latter consists of two elementary trusses that, on their own, act as mechanisms, but together produce a stiff structure.

The elastic properties were computed by finite element (FE) analysis. The FE mesh was created using linear Euler-Bernoulli beam elements, suitable for small-strain analyses with small rotations. The strut slenderness ratio,  $\ell/2r$ , was selected to be 25, the linear number of unit cells was  $n=25$ , and the constituent elastic properties were taken to be: Young's modulus,  $E_0=200$  GPa, and shear modulus,  $G_0=80$  GPa. The strut connections at the nodes were taken to be rigid. Nodal displacements were applied in two configurations, subjecting the trusses to a state of uniaxial compression parallel to one of the principal truss directions (denoted 1) or pure shear (in the 1–2 plane). The reaction forces needed to maintain the prescribed nodal displacements on the external faces were computed and used to determine the global elastic constants: Young's modulus  $E_l$ , Poisson's ratio  $\nu_{12}$ , and shear modulus  $G_{12}$ , as well as the elastic anisotropy parameter  $\omega \equiv 2G_{12}(1 + \nu_{12})/E_l$  (Nye, 1985). The results are summarized in Table 5. The FE results were also used to construct polar plots of the Young's modulus for all possible uniaxial loadings. Sections through these plots along (011) planes are shown in Fig. 8. (This plane contains directions along the body edge, the face diagonal and the body diagonal.) For reference, the theoretical upper bound ( $E/\rho E_0 = 1/6 \approx 0.167$ ) for isotropic trusses is also shown.

By comparison to the properties of the  $\{nFCC\}^3$  truss, the Young's modulus of the compound truss is greater, its shear modulus is only slightly lower, and its anisotropy parameter  $\omega$  is closer to unity. The higher degree of isotropy of the compound truss is also evident in the polar plot in Fig. 8; the Young's modulus of the compound truss falls in the narrow range of 0.161–0.170 (consistently close to the upper bound) whereas that of the  $\{nFCC\}^3$  truss varies over the range 0.111–0.200. Thus, for applications in which both high specific stiffness and isotropy are sought, the compound truss would be the preferred choice.

## 7. Concluding discussion

We have presented a system for classification and taxonomy of periodic truss structures. The system employs concepts from crystallography and geometry to describe nodal locations and connectivity of struts. The conventions and terminology yield concise yet unambiguous descriptions of structure types and of specific truss structures. The system captures a broad range of trusses that have been studied in various science and engineering fields and could be expanded to include

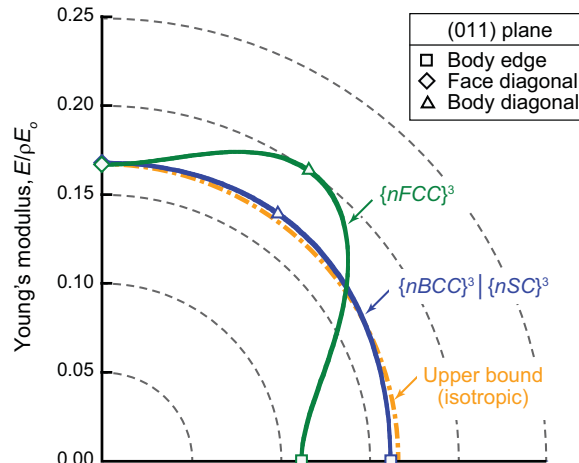


**Fig. 8.** Planar sections through polar plots of Young's modulus along the (011) plane for the elementary  $\{nFCC\}^3$  and the compound  $\{nBCC\}^3 | \{nSC\}^3$  trusses. The abscissa is aligned with one of the body edges. Because of symmetry, results for only one quadrant are presented. Results are based on FEA for  $n=25$ .

structures with even greater complexity, going beyond the cases considered here. Additionally, the *FE* results demonstrate that the  $\{nBCC\}^3|\{nSC\}^3$  compound truss exhibits elastic properties that rival those of  $\{nFCC\}^3$ , especially when isotropy is a determining factor.

Numerous trusses that have been studied in recent years do not appear to be particularly well-suited for use as stiff and strong lightweight structures on their own. Specifically, those based on the elementary structure types  $\{SC\}$ ,  $\{BCC\}$ ,  $\{BCT\}$ ,  $\{ST\}$  and  $\{R\}$  exhibit mechanisms and would not be expected to be significantly better than comparable stochastic foams. However, when combined with other structural elements, such as face sheets to make a sandwich panel, the additional constraints may, in some cases, suppress collapse modes and render the trusses stiff and strong. Examples include sandwich panels with truss cores of  $1/2\{nBCT\}^2\langle 1 \ 1 \ \lambda_z \rangle$  (single-layered pyramidal) or  $1/3\{nR\}^2\langle 1 \ 1 \ \lambda_z \rangle$  (tetrahedral). Their performance is attributable in part to the fact that all struts are affixed to both face sheets without any intervening nodes. By introducing additional nodes, the cores become progressively weaker, especially in the near-edge regions of the panels where the constraints are low. This would occur, for example, if a  $1/2\{nBCT\}^2\langle 1 \ 1 \ \lambda_z \rangle$  core were replaced with a  $5\{nBCT\}^2\langle 1 \ 1 \ \lambda_z \rangle$  core (with a proportionate ten-fold reduction in strut dimensions to preserve core thickness).

Finally, although the principal motivation for studying the elastic properties of the  $\{nBCC\}^3|\{nSC\}^3$  truss was to ascertain the extent to which the deficiencies in the two constituent elementary trusses could be mitigated by compounding, we find that the compound truss is (coincidentally) closely related to the one that Gurtner and Durand (2014) recently identified as the stiffest isotropic truss. In our terminology, the latter structure type is  $\{BCC\}|\{SC\}|\{SC\}|[1/21/21/2]$ . It is a compound truss that naturally emerged from our classification system; a specific example is shown in Fig. 3(b). Interestingly, the somewhat simpler compound truss for which elastic properties were calculated in the present study proves to be essentially as good as the stiffest isotropic truss, as evidenced by the polar plot of Young's modulus in Fig. 8. In light of these observations, one might expect that, by systematically stepping through and analyzing the finite number of structure types identified through the present classification system, optimal structures for prescribed mechanical and functional requirements could be ascertained in an expeditious manner.

## Acknowledgments

This work was supported by the Institute for Collaborative Biotechnologies through Grant W911NF-09-0001 from the US Army Research Office. The content of the information does not necessarily reflect the position or the policy of the Government, and no official endorsement should be inferred.

## References

- Bauer, J., Hengsbach, S., Tesari, I., Schwaiger, R., Kraft, O., 2014. High-strength cellular ceramic composites with 3D microarchitecture. *Proc. Nat. Acad. Sci.* 111, 2453.
- Bernal-Ostos, J., Rinaldi, R.G., Hammetter, C.I., Stucky, G.D., Zok, F.W., Jacobsen, A.J., 2012. Deformation stabilization of lattice structures via foam addition. *Acta Mater.* 60, 6476.
- Bückmann, T., Stenger, N., Kadic, M., Kaschke, J., Fröhlich, A., Kennerknecht, T., Eberl, C., Thiel, M., Wegener, M., 2012. Tailored 3D mechanical metamaterials made by dip-in direct-laser-writing optical lithography. *Adv. Mater.* 24, 2710.
- Cheng, X.Y., Li, S.J., Murr, L.E., Zhang, Z.B., Hao, Y.L., Yang, R., Medina, F., Wicker, R.B., 2012. Compression deformation behavior of Ti-6Al-4V alloy with cellular structures fabricated by electron beam melting. *J. Mech. Behav. Biomed. Mater.* 16, 153.
- Chiras, S., Mumm, D.R., Evans, A.G., Wicks, N., Hutchinson, J.W., Dharmasena, K., Wadley, H.N.G., Fichter, S., 2002. The structural performance of near-optimized truss-core panels. *Int. J. Solids Struct.* 39, 4093.
- Deshpande, V.S., Fleck, N.A., Ashby, M.F., 2001. Effective properties of the octet-truss lattice material. *J. Mech. Phys. Solids* 49, 1747.
- Doty, R.E., Kolodziejska, J.A., Jacobsen, A.J., 2012. Hierarchical polymer microlattice structures. *Adv. Eng. Mater.* 14, 503.
- Evans, A.G., Hutchinson, J.W., Fleck, N.A., Ashby, M.F., Wadley, H.N.G., 2001. The topological design of multifunctional cellular metals. *Prog. Mater. Sci.* 46, 309.
- Gibson, L.J., Ashby, M.F., 1997. In: *Cellular Solids: Structure and Properties* 2nd ed. Cambridge University Press, Cambridge.
- Gilman, J.J., Tetrahedral truss, US Patent 4,446,666, 1984.
- Gurtner, G., Durand, M., 2014. Stiffest elastic networks. *Proc. R. Soc. A* 470, 20130611.
- Hammetter, C.I., Rinaldi, R.G., Zok, F.W., 2012. Periodic truss lattices for high strength and energy absorption. *J. Appl. Mech.* 80, 041015.
- Hutchinson, R.G., Wicks, N., Evans, A.G., Fleck, N.A., Hutchinson, J.W., 2003. Kagome plate structures for actuation. *Int. J. Solids Struct.* 40, 6969–6980.
- Jacobsen, A.J., Barvosa-Carter, W., Nutt, S., 2007. Micro-scale truss structures formed from self-propagating photopolymer waveguides. *Adv. Mater.* 19, 3892.
- Jacobsen, A.J., Barvosa-Carter, W., Nutt, S., 2007. Compression behavior of micro-scale truss structures formed from self-propagating polymer waveguides. *Acta Mater.* 55, 6724.
- Jacobsen, A.J., Barvosa-Carter, W., Nutt, S., 2008. Micro-scale truss structures with three-fold and six-fold symmetry formed from self-propagating polymer waveguides. *Acta Mater.* 56, 2540.
- Kang, K.J., 2015. Wire-woven cellular metals: the present and future. *Prog. Mater. Sci.* 69, 213–307.
- Kraft, R.W., Construction arrangement, US Patent 3,139,959, 1961.
- Li, S.J., Xu, Q.S., Wang, Z., Hou, W.T., Hao, Y.L., Yang, R., Murr, L.E., 2014. Influence of cell shape on mechanical properties of Ti-6Al-4V meshes fabricated by electron beam melting method. *Acta Biomater.* 10, 4537.
- Lucato, S.L.S., Wang, J., Maxwell, P., McMeeking, R.M., Evans, A.G., 2004. Design and demonstration of a high authority shape morphing structure. *Int. J. Solids Struct.* 41, 3521–3543.
- Murr, L.E., Amato, K.N., Li, S.J., Tian, Y.X., Cheng, X.Y., Gaytan, S.M., Martinez, E., Shindo, P.W., Medina, F., Wicker, R.B., 2011. Microstructure and mechanical properties of open-cellular biomaterials prototypes for total knee replacement implants fabricated by electron beam melting. *J. Mech. Behav. Biomed. Mater.* 4, 1396.
- Murr, L.E., Gaytan, S.M., Medina, F., Lopez, H., Martinez, E., Machado, B.I., Hernandez, D.H., Martinez, L., Lopez, M.I., Wicker, R.B., Bracke, J., 2010. Next-generation biomedical implants using additive manufacturing of complex, cellular and functional mesh arrays. *Philos. Trans. R. Soc. A* 368, 1999.

- Nye, J.F., 1985. Physical Properties of Crystals. Clarendon Press, Oxford, UK (Chap VIII).
- Pettermann, H.E., Husing, J., 2012. Modeling and simulation of relaxation in viscoelastic open cell materials. *Int. J. Solids Struct.* 49, 2848.
- Rathbun, H.J., Wei, Z., He, M.Y., Zok, F.W., Evans, A.G., Sypeck, D.J., Wadley, H.N.G., 2004. Measurement and simulation of the performance of a lightweight metallic sandwich structure with a tetrahedral truss core. *J. Appl. Mech.* 71, 368.
- Wadley, H.N.G., 2000. Multifunctional periodic cellular metals. *Philos. Trans. R. Soc. A* 364, 31.
- Wadley, H.N.G., Fleck, N.A., Evans, A.G., 2003. Fabrication and structural performance of periodic cellular metal sandwich structures. *Compos. Sci. Technol.* 63, 2331.
- Wainwright, S.A., Briggs, W.D., Currey, J.D., Gosline, J.M., 1982. Mechanical Design in Organisms. Princeton University Press, Princeton, New Jersey.
- Wallach, J.C., Gibson, L.J., 2001. Mechanical behaviour of a three-dimensional truss material. *Int. J. Solids Struct.* 38, 7181.
- Weaire, D. (Ed.), 1996. The Kelvin Problem: Foam Structures of Minimal Surface Area. Taylor and Francis, London, UK.
- Wicks, N., Hutchinson, J.W., 2001. Optimal truss plates. *Int. J. Solids Struct.* 38 (30–31), 5165–5183.